ASYMMETRICAL HETEROATOM SUBSTITUTIONS IN THE INDENOFLUORENE FRAMEWORK: SYNTHESIS AND CHARACTERIZATION OF 4,10-DIMESITYLBENZO[5,6]-S-INDACENE[1,2-B]THIOPHENE AND 5,11-DIMESITYLBENZO[5,6]-S-INDACENE[1,2-B]THIOPHENE

by

NATHANIEL J. O'NEAL

A THESIS

Presented to the Department of Chemistry and Biochemistry
and the Robert D. Clark Honors College
in partial fulfillment of the requirements for the degree of
Bachelor of Science

May 2015

An Abstract of the Thesis of

Nathaniel J. O'Neal for the degree of Bachelor of Science
in the Department of Chemistry and Biochemistry to be taken June 2015

Title: Asymmetrical Heteroatom Substitutions in the Indenofluorene Framework: Synthesis and Characterization of 4,10-Dimesitylbenzo[5,6]-s-indacene[1,2-b]thiophene and 5,11-Dimesitylbenzo[5,6]-s-indacene[1,2-b]thiophene

Approved: _____

Professor Michael M. Haley

This project describes the synthetic method for production of asymmetrical indenofluorenes. The method presented allows for broad yet selective asymmetric substitution on the indenofluorene framework and provides a basis for future asymmetric indenofluorene derivatives. As proof of concept, this project synthesized and characterized 4,10-dimesitylbenzo[5,6]-s-indacene[1,2-b]thiophene and 5,11-dimesitylbenzo[5,6]-s-indacene[1,2-b]thiophene. Asymmetrical indenofluorenes have potential use as n-type organic semiconductors. As such, the structural, optical, and electronic properties of these compounds have also been analyzed and reported. Additionally, this project led to the creation of several compounds hitherto undescribed in the literature.

Acknowledgements

This project was supported by Award Number CHE-1301485 from the National Science Foundation.

I would like to thank Professor Michael M. Haley for graciously providing me with the opportunity to perform first hand research. This project would not have been possible without his support, nor would this project have been successful without the help and mentorship of Jonathan L. Marshall, whose help I have greatly appreciated. Gratitude is also owed to Gabriel E. Rudebusch and Conerd K. Frederickson for their aid and support in the laboratory. In addition, I would also like to thank Dr. S. Michael Strain and the CAMCOR staff for support with NMR Spectroscopy for this project, as well as Dr. Lev N. Zahkarov and his masterful use of XRD for this project.

I would also like to thank Professor Terry L. Hunt and Miriam Jordan for their help and guidance through the Robert D. Clark Honor's College thesis process.

My friends and family are also deserving of my thanks, they are the ones who have encouraged me through this project and all its ups and downs.

Table of Contents

List of Figures

List of Tables

Introduction

Technology is always looking for the next best thing. In today's economy, riddled with electronics, that means the search for more efficient devices. Whatever the device — light emitting diodes, field effect transistors, or photovoltaics — they are all made possible using semiconductors. This has turned the gaze of many towards the search for more efficient semiconductors.

Semiconductors can be used in a variety of ways, all of which revolve around electron transfer. Removal of electrons generates a positive charge on the semiconductor that is known as a "hole"; these are appropriately named p-type semiconductors. The addition of electrons places a negative charge on the semiconductor; these are called n-type semiconductors (1). The majority charge carrier, "holes" or electrons, determines if a compound is p-type or n-type (1).

Historically, most semiconductors are made using silicon. These are doped to produce p-type or n-type characteristics. Doping involves the addition of elements that are either electron rich or electron poor into the silicon structure (2). Silicon semiconductor synthesis, however, is an energy intense process that involves the heating of silicon to extremely high temperatures, usually in excess of 1450 °C for extended periods of time (3).

These harsh conditions and high costs have resulted in a lot of focus towards organic semiconductors (OSCs). Compared to silicon, OSCs are much easier to solvate, which opens up less energy intensive reactions for both compound synthesis and device fabrication (1, 4)**.** Many organic synthesis steps never exceed 150 °C and often reactions can be performed at room temperature (5, 6). These differences make OSC

synthesis and device production a potentially simpler and more cost effective alternative to inorganic semiconductors.

Background

Basic Principles

Before we can understand OSC design, we first need to understand electrons. Electrons inhabit orbitals around the nucleus of atoms. Each of these orbitals has a designated energy level. When two atoms bond together, these orbitals interact to essentially "share" electrons (4). During this electron sharing, the electrons occupy the lowest energy orbitals available. This is because the lower in energy the orbital, the more stable the electrons are in that position (7). We can easily understand differences in orbital energies by looking at the periodic table (Figure 1). When moving down a column in the periodic table, each element's electrons are filling orbitals of a higher energy than the element above it (4); therefore, when elements bond together, their orbitals mix and their electrons fill the lowest energy orbitals available.

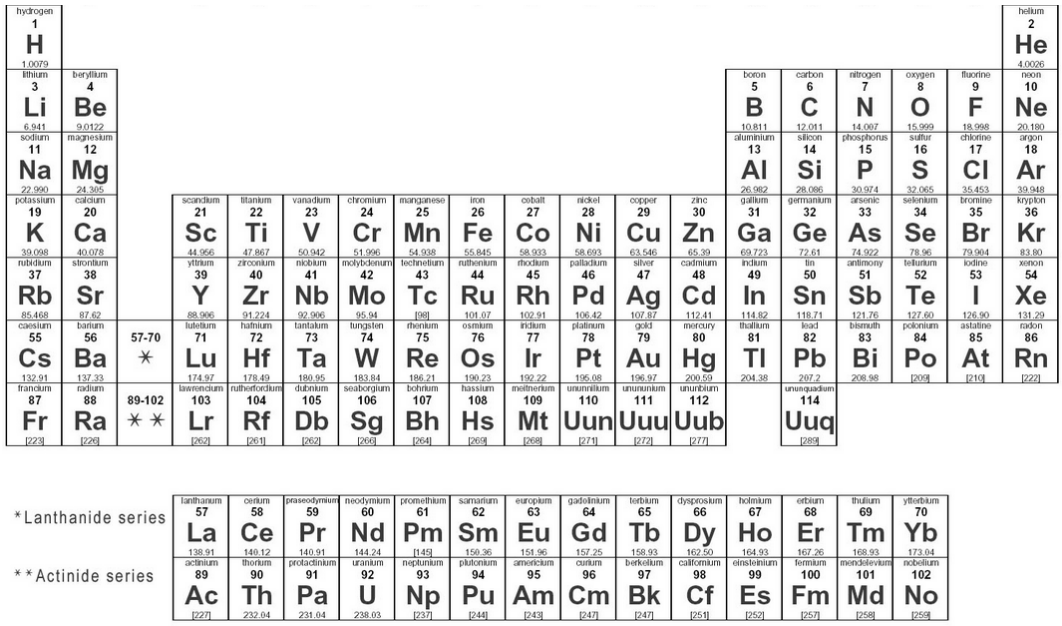

Figure 1: Periodic Table of the Elements (1').

Furthermore, only valence electrons participate in bonding. These are the electrons that inhabit the outermost orbitals of a given atom. In Figure 1, we can count valence electrons by counting from the beginning of an element's row until we arrive at the desired element (4). Depending on how many valence electrons atoms have when bonding, there might not be enough to fill an orbital. When this occurs, it becomes very easy for a compound to conduct electrons through that partially filled orbital. This is known as being metallic and is what occurs in conducting compounds (8). When electrons fill an orbital and there are not enough to partially fill the next orbital, then a band gap is created. This is the energy difference between the highest occupied molecular orbital (HOMO) and the lowest unoccupied molecular orbital (LUMO). These levels are also known as the valence band and the conduction band, respectively (9). The level of this energy gap determines if a compound is a semiconductor or not. If

a compound has a band gap greater than 0 eV to approximately 4.0 eV in energy, then it can be considered a semiconductor. When the band gap exceeds 4.0 eV, it becomes too impractical to get electrons into the conduction band; these compounds are known as insulators (8).

For silicon semiconductors, electrons are transferred across the band gap through the electron rich or deficient dopants that have been added (2). OSCs do not conduct electrons through the same process. Instead, organic molecules conduct electrons through a secondary set of orbitals that lie perpendicular to the bonding orbitals (Figure 2) (9).

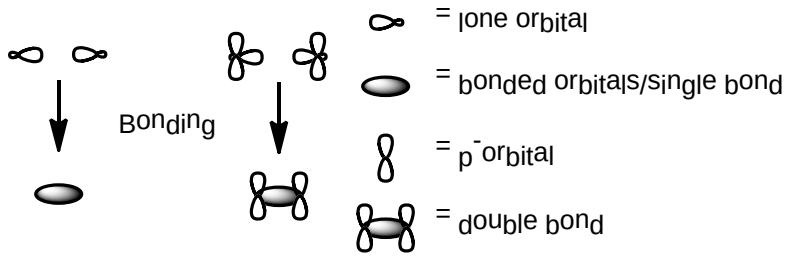

Figure 2: Bonding scheme of two atoms interacting to achieve orbital overlap for both single and double bonds.

When bonded, two atoms are sharing electrons between them. The amount of electron density being shared between the two atoms determines the strength and length of that bond (4). When only one orbital from each atom are interacting, the resulting bond is known as a single bond. If two atoms are in the right orientation, then their p-orbitals can also have some interaction. In this interaction, a small amount of electron density can be added to the bond between the atoms. This generates more electron density and results in a shorter and stronger bond (10). Colloquially, we refer to this as a double bond or pi bond and represent it with doubled lines (Figure 3).

Figure 3: Stick model of 2-butene. Each line depicts a single bond. Each end of a connected line segment represents a carbon. The double line is indicative of a double bond. Every carbon has a total of four bonds. The bonds not shown are hydrogens and they are omitted in these diagrams for clarity, but assumed present.

Organic molecules can transfer electrons across these double bonds, through their p-orbitals; therefore, in order to transfer electrons, OSCs need to have these double bonds throughout their molecular structure. When these double bonds are linked it is known as conjugation (10). Traditionally, we represent conjugation by the separation of double bonds (Figure 4).

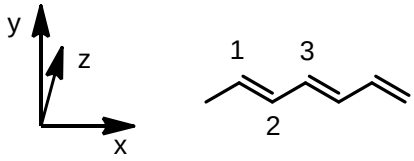

Figure 4: Axis for orientation (left) Stick model of 1,3,5-heptatriene depicting the conjugation of double bonds in organics (right).

1,3,5-Heptatriene (shown in Figure 4), however, is not necessarily efficient at transferring electrons throughout its conjugated pi system. This is because even if a molecule has conjugation, the orbitals also have to be in alignment with one another in order to transfer electrons between compounds. In this molecule, there is free rotation around the single bonds. Since the p-orbitals are perpendicular to the single bonds, it is unlikely that they will all be aligned properly (10). For example, the p-orbitals at site 1 could be along the x-axis while the p-orbitals at site 2 could be along the y-axis. In some OSCs, these p-orbitals are forced into alignment via formation of a cyclic molecule (Figure 5).

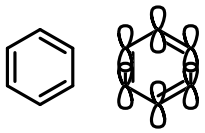

Figure 5: Stick model of benzene (left) with p-orbitals shown (right). Given the angle of the benzene ring the p-orbitals would be protruding through the page.

With this model, we can transfer electrons through the pi system (the conjugated p-orbitals) of the compound.

Aligned p-orbitals and a HOMO–LUMO gap of less than 4 eV, however, are still not enough for a successful OSC. To be successful, an individual molecule needs to be able to not only transfer electrons intra-molecularly, but also inter-molecularly through a network of its neighboring molecules. This can only occur if the p-orbitals of nearby molecules are within the Van der Waal's radius (9). Once inside this radius, the p-orbitals of two neighboring molecules become close enough to be able to interact and transfer electrons. For carbon–carbon p-orbital interactions, the Van der Waal's radius is 3.4 angstroms (Å), or 0.34 nm (9). For two benzene rings to pass electrons inter-molecularly through their pi systems, they would have to be within 3.4 Å and in the right orientation.

Because of these interactions, we are interested in how potential OSC compounds stack in 3-dimensional space. Since these cyclic organic molecules have their p-orbitals perpendicular to the plane of the molecule, we are mostly interested in face-to-face stacking arrangements (Figure 6). Through this stacking motif, we get maximum potential for p-orbital interaction of neighboring molecules. Although there are a variety of stacking motifs, some of the most prevalent are the "herringbone" and

the “brick and mortar” style packing (Figure 6) (11). Of these two motifs, the most efficient for electron transfer is the “brick and mortar”.

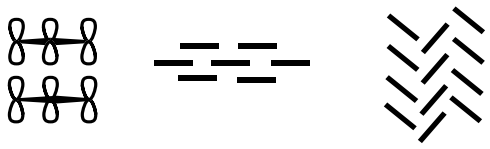

Figure 6: Desired orientation for p-orbitals of cyclic organics during stacking (left). “Brick and mortar” style packing (middle). “Herringbone” style packing (right). The p-orbitals are not shown in the stacking models for clarity but would be perpendicular to the line segments.

Characterization Techniques

During synthesis of a molecule, a variety of techniques are used to definitively characterize the compound and analyze its optical and electronic properties. The most common technique for structural characterization of organic compounds is ^{1}H nuclear magnetic resonance spectroscopy (NMR). NMR uses a magnetic field to align the nuclear spins of the hydrogen atoms in a molecule. This magnetic field is then perturbed using radio wave pulses. Depending on where the hydrogens are in a molecule, they will behave differently in the magnetic field and produce unique resonance frequencies (12). Each distinct signal is measured and relayed onto a spectrum. A Fourier transform can be used to interpret these signals by “decomposing” a signal into its constituent frequencies (12). Using this technique, we can interpret the frequencies of the chemically distinct hydrogens and determine the location and number of hydrogens in a compound (Figure 7) (10).

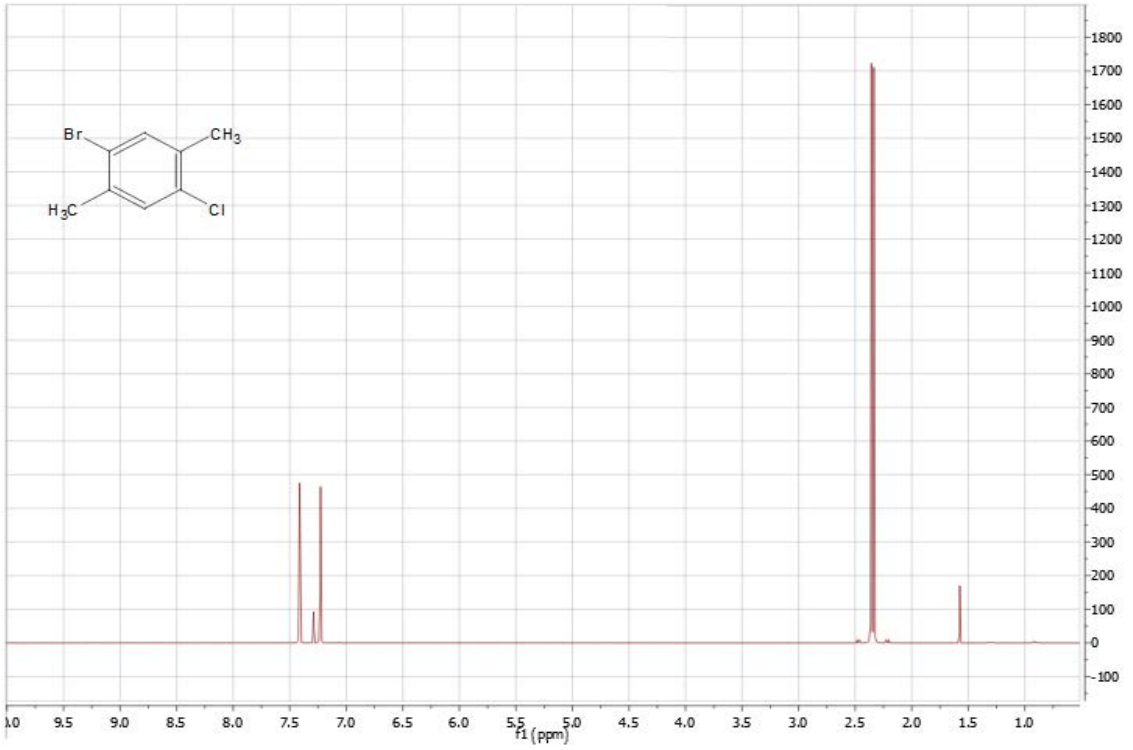

Figure 7: ^{1}H NMR spectrum of 2-bromo-5-chloro-1,4-xylene. Chemical shift is along the x-axis (ppm) and signal intensity along the y. Each peak represents a chemically unique hydrogen. The larger the peak the more hydrogens are in that position. Three peaks on the left represent the hydrogens on the center ring and the solvent peak. The large two peaks show the methyl hydrogens. The peak at the right is residual water.

When characterizing a new compound, ^{13}C NMR analysis is also used. ^{13}C NMR determines the chemical environment of the carbons present in the structure. Like ^{1}H NMR, this technique can be used to determine chemical structure. ^{13}C NMR collection is still ongoing for the compounds presented in this thesis.

When compounds require physical and optoelectronic property readings, x-ray crystallography, ultraviolet and visible light spectroscopy (UV/Vis), and cyclic voltammetry (CV) are used. X-ray crystallography uses x-ray diffraction (XRD). In this method, a single crystal of a compound is placed onto a diffractometer which shoots a beam of x-rays at the crystal. The electrons in the compound diffract the x-rays,

allowing for a diffraction measurement. Based off of the angles and intensities of the diffracted beams, the average positions of atoms and bonds within the crystal can be determined (8). This provides an understanding of how the atoms in the molecules are interacting. It gives evidence of bond distances as well as how the molecules pack together. XRD for organic compounds allows us to determine if a compound's molecules are in the right orientation and if they are stacked close enough together have inter-molecular electron transfer.

CV measures the oxidation and reduction potential of a compound in solution. In other words, this tells us how a compound gains and loses electrons. This is performed through a process in which an electrode's voltage is increased linearly over time. When a set potential is reached, the voltage is turned back down until the system returns to the starting potential (13). The voltage is then plotted as the current through the electrode vs. potential (Figure 8).

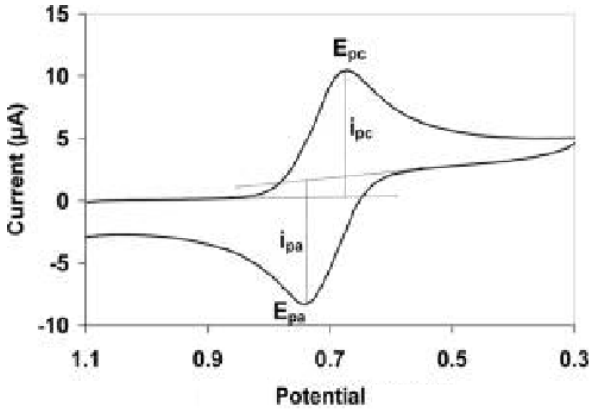

Figure 8: Cyclic voltammetry data showing current vs. potential (2').

In potential OSC compounds, we expect to see reversible reductions and oxidations. This shows that the compound can reversibly gain and lose electrons (or

vice-versa) without any change to the chemical structure of the molecule. A chemical change would be seen if once a potential was reached, it could not be returned to. Without being reversible, any potential capacity a compound has as an OSC would be lost. A compound that does not show reversibility would have little to no application for use in a device. Furthermore, the oxidation and reduction potentials are used to experimentally determine the HOMO/LUMO levels of a compound (14).

UV/Vis spectroscopy can be used to determine the optical properties of a compound. Normally, electrons are in a resting state. When the proper amount of energy is applied, an electron can "jump" from its orbital into a higher energy orbital before relaxing back down. This occurs when the electrons receive enough energy to cross the band gap, allowing them to enter the orbitals at or above the conduction band (9). UV/Vis spectrometers can measure these energies by shining a spectrum of light at a sample. The light ranges from ultraviolet through the visible light spectrum. The different wavelengths of light all have different energies. Any wavelength of light that can excite an electron will be absorbed by the compound. The light that does not excite any electrons passes through the compound and is read by the spectrometer. From this data, we can produce a graph showing the efficiency of absorption of a compound vs. wavelength (10). The maximum absorbance of a compound is referred to as lambda-max ($\lambda_{max)}$. Using λ_{max}, we can estimate the amount of energy needed to excite an electron. This energy value can be used to estimate LUMO levels. We can also use the data to calculate the energy gap between the valence and conduction bands (9, 14). Generally, the higher the λ_{max} the lower the LUMO and the more potential a compound has for semiconducting performance.

Using these analytical techniques, we can characterize a compound and determine its structural, optical, and electronic properties. Although there are methods to predict HOMO–LUMO levels and to align the p-orbitals via cyclization, there are currently no means to predict the stacking pattern of organic compounds. Therefore, it is necessary to produce a variety of molecular scaffolds that offer multiple tuning sites. These sites allow for molecular tweaks in order to adjust the molecule's electronic properties and stacking in the solid state. It is the goal of this thesis to present the synthesis and characterization of a novel scaffold that can be used for future research of potential OSC compounds.

History

These prerequisites of conjugation and optimal HOMO/LUMO levels have led the majority of OSC research towards polycyclic aromatic hydrocarbons (PAHs) and polyarenes. One of the most widely researched PAHs due to its HOMO/LUMO levels, packing in the solid state, and optoelectronic properties, is pentacene, a fully conjugated five ring fused system (Figure 9) (6, 11).

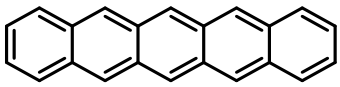

Figure 9: Stick model of pentacene.

Pentacene as well as many of its derivatives behave as p-type compounds. As a whole, research into pentacene and similar PAHs has furnished a myriad of organic p-type compounds. This research has contributed greatly to our understanding and synthetic

knowledge about potential OSCs, but has left a dearth of available n-type organic compounds in its wake (6, 15). At the University of Oregon, however, a new n-type scaffold has excited research, the indenofluorene (IF) (Figure 10).

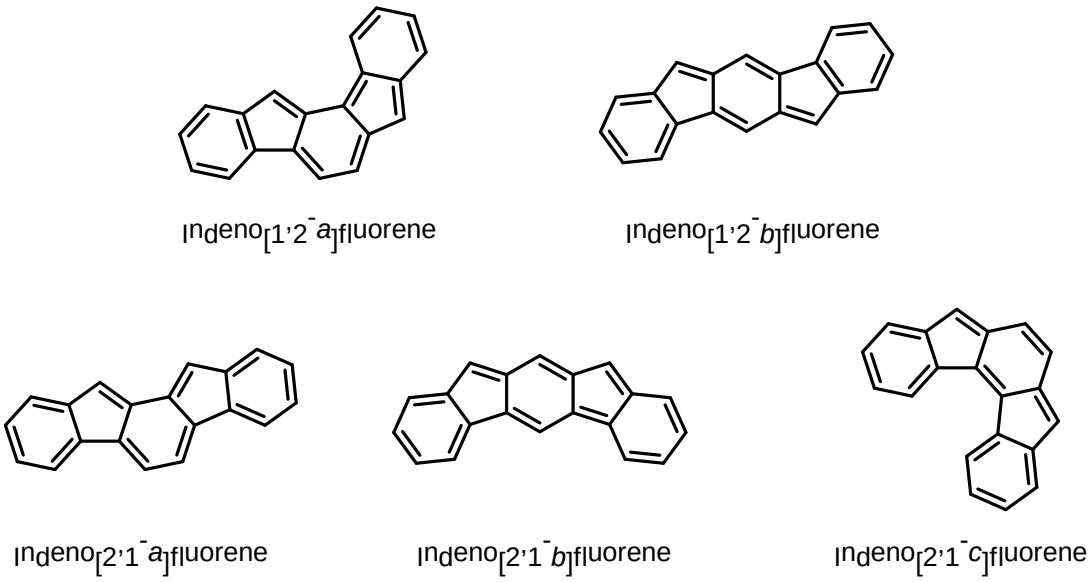

Figure 10: Five isomers of indenofluorenes.

There are 5 different isomers of the IF skeleton, of which the first IF was synthesized by Gabriel in 1884 (16). It was not until the 1950s, however, that indenofluorene synthesis was revived by Chardonnen and Deuschel to afford multiple derivatives of this compound (17, 18). Later, Swager and Komatsu prepared and investigated the semiconducting potential of the [1,2-b] IF dione (19, 20). In the early 2000s, Wang et al. pioneered a simple and effective means for synthesizing IFs through Suzuki cross-coupling reactions (Figure 11) (21). This route opened up new possibilities for efficient synthesis of [1,2-b] IF derivatives. Due to the [1,2-b] IF's remarkable

electronic properties, stability, and ease of synthesis, it has become the most studied isomer of the IF family (6).

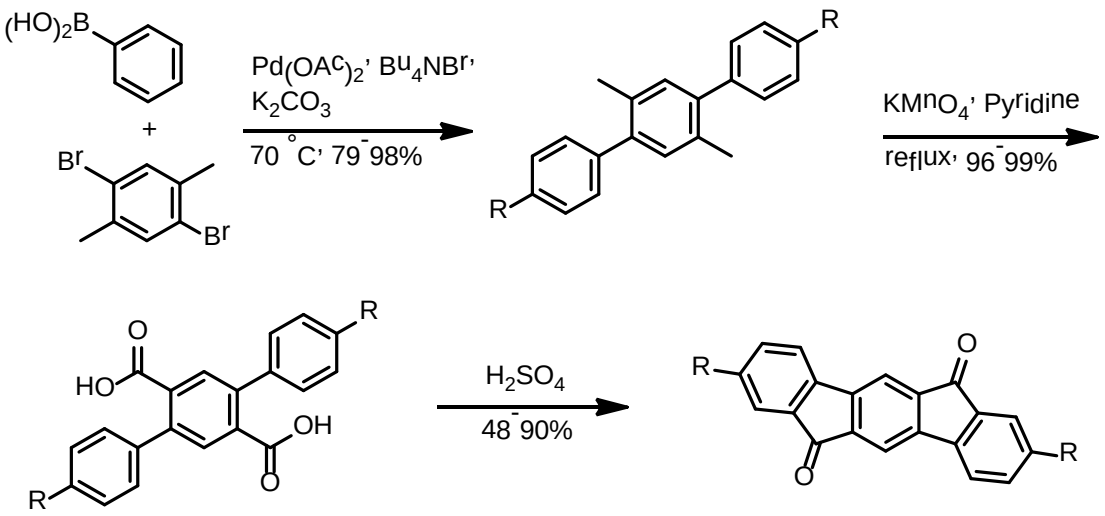

Figure 11: Synthesis of IFs using Suzuki cross-coupling.

Functionalization

Previous research on pentacene was also performed to combat instability of the molecule towards oxidative and photolytic degradation (Figure 12) (11).

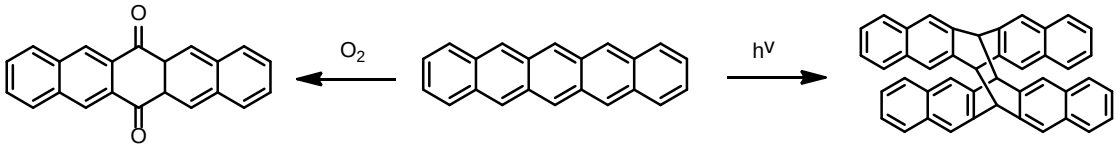

Figure 12: Degradation products of pentacene via oxidative degradation (left) and photolytic degradation (right).

One of the first functionalization strategies used was the appendage of simple phenyl substituents to the perimeter of the pentacene, in order to tune the structural configuration and improve stability (Figure 13) (11).

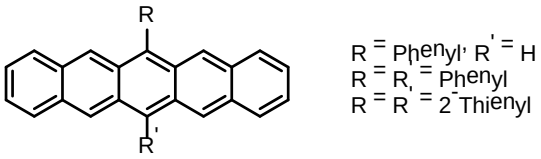

Figure 13: Aryl-functionalized pentacene.

This research inspired the Haley group to attempt similar tuning of the [1,2-b] IF, leading to the production of a variety of [1,2-b] IFs substituted at various positions (Figure 14) (22, 23).

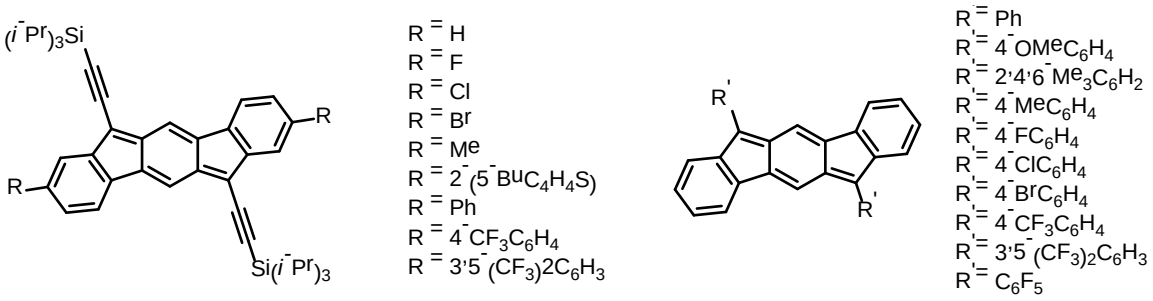

Figure 14: IF derivatives with various sterically bulky groups or electron withdrawing groups appended at the 2 and 8 positions (left), 6 and 12 positions (right).

As expected, the sterically bulky groups also stabilized the fully conjugated [1,2-b] IF. Optical analysis of these derivatives revealed a correlation between appendage site and λ_{max}. Substitution at the 2 and 8 positions had very little impact on absorption profiles with λ_{max} between 561-577 nm, with substitution at the 6 and 12 positions showing a wider variation of λ_{max} from 533–607 nm (6). The higher potential λ_{max} is of interest because it can mean a lower LUMO and smaller band gap when substituting at the 6 and 12 positions as opposed to the 2 and 8 positions (9). Electronic analysis also showed favorable HOMO and LUMO energies, between 5.5 and 5.8 eV

and 3.6 to 4.0 eV, respectively for the 6 and 12 substituted derivatives (23). With LUMO levels below 4 eV, these molecules show potential as OSCs (8).

In addition to stabilization by the appendage of sterically bulky groups, pentacene was also stabilized via thieno fusion. In this technique, the outer rings of the pentacene skeleton were substituted for thiophenes, a five membered ring consisting of four carbons and one sulfur. The resulting compound showed reduced susceptibility to oxidative and photolytic degradation as well as a lower energy gap (11). With this in mind, Haley et al. synthesized both isomers of indacenedithiophene (IDT), a structural analogue of the indenofluorenes (Figure 15) (15).

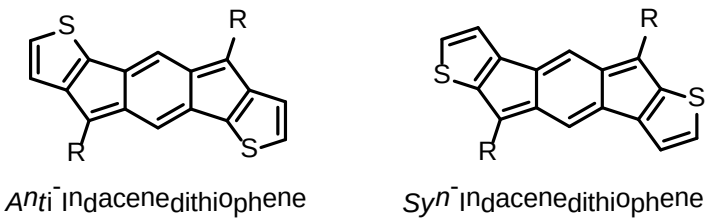

Figure 15: *Anti- and syn-* isomers for the fully reduced indacenedithiophenes.

As expected, the IDTs showed a destabilized HOMO and stabilized LUMO compared to the IFs, resulting in a lower band gap than the [1,2-b] IF (15). Through substitution of steric bulky groups or electron withdrawing groups at the "R" position, as well as heteroatom substitution such as thieno fusion, the Haley group showed that one can easily tune the stability and electronic properties of the [1,2-b] IF scaffold.

New Approach

To further explore molecular tuning of the IFs, it was hypothesized that judicious choice of these substitutions could be performed to furnish asymmetrical IF

derivatives. The idea, would be to place an electron donor on one end and an electron acceptor on the opposite end of a molecule. It is well known that molecules often adopt conformations that maximize interactions between good donor orbitals and good acceptor orbitals (9). Through these interactions, an asymmetrical IF could have unique electronic properties.

To date, there are currently no synthetic means to produce asymmetrical IF derivatives. This thesis presents a methodology that allows for broad asymmetric substitution to the IF core. As proof of concept, I have synthesized and characterized the first asymmetrical IFs, 4,10-dimesitylbenzo[5,6]-s-indacene[1,2-b]thiophene (*anti*-BIT) and 5,11-dimesitylbenzo[5,6]-s-indacene[1,2-b]thiophene (*syn*-BIT) (Figure 16).

Figure 16: *Syn*- and *anti*- conformations of potential asymmetrical compounds.

Culminating ideas from previous research, the BITs have sterically bulky groups substituted at the 6 and 12 positions to stabilize the fully conjugated molecules. Moreover, a single thieno fusion further stabilizes the BIT, and places the molecule between the [1,2-b] IF and the IDTs chemically, allowing for easy comparison of electronic properties.

Although not boasting strong electron donors and acceptors, the BITs potentially offer some unique properties that could stem from having a dipole. Sulfur, being more electronegative than carbon, can pull electron density through the conjugated system

leaving a small negative charge near the sulfur; this is referred to as a dipole (10). As a consequence, the carbons on the other side of the BIT would have less electron density leaving them with a positive dipole. Charge-charge interactions between the positive and negative dipoles of adjacent molecules could align the molecules for a more optimal rearrangement in the solid state. These interactions could potentially align the molecules into a “brick and mortar” style packing and allow for optimal orientation for orbital overlap. Moreover, the slight dipole should increase the solubility of BITs in polar solvents, thus increasing the ease of fabrication for these compounds as well as possible future devices. This is because when a molecule can be solvated, it has a higher probability of interacting with other compounds in solution. This allows for faster reactions and more efficient synthesis. Improved solubility is a useful addition when working with oxidized IF cores (known as diones), notorious for their insolubility.

Synthesis

Synthesis of the fully reduced BITs began with variation of the previous synthesis used to make the [1,2-b] IF and the synthesis of the indacenedithiophenes (15, 22). The former made use of Suzuki cross-coupling reactions (Figure 12), while the latter made use of Stille cross-coupling (Figure 17).

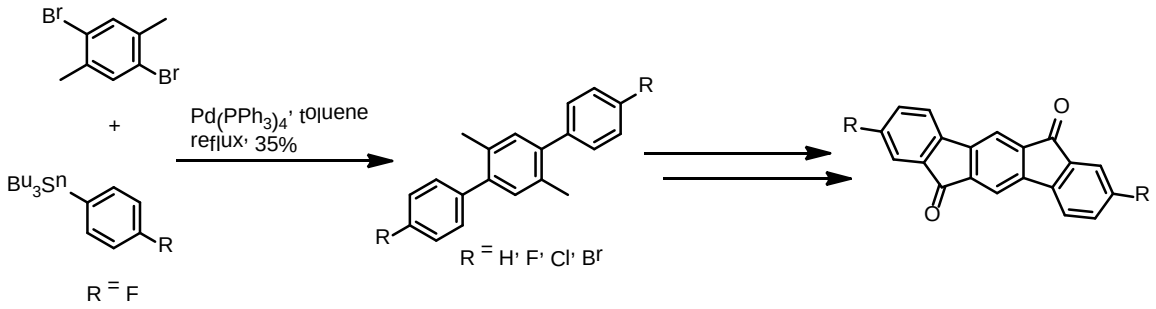

Figure 17: Generic synthetic scheme for Stille cross-coupling. Stannane (bottom left) is used instead of the boronic acid used in Suzuki cross-coupling reactions.

Suzuki cross-coupling was chosen over the Stille cross-coupling because boronic acids are safer to work with than the highly toxic stannanes required for Stille reactions. It should be noted, that preliminary research into asymmetric IFs suggests Stille cross-coupling can so also be used. This is further supported by its use in the synthesis for the IDTs (15). Although many methodologies presented in the literature were used, the majority of the compounds presented in this thesis have not been reported in the literature (Figure 18).

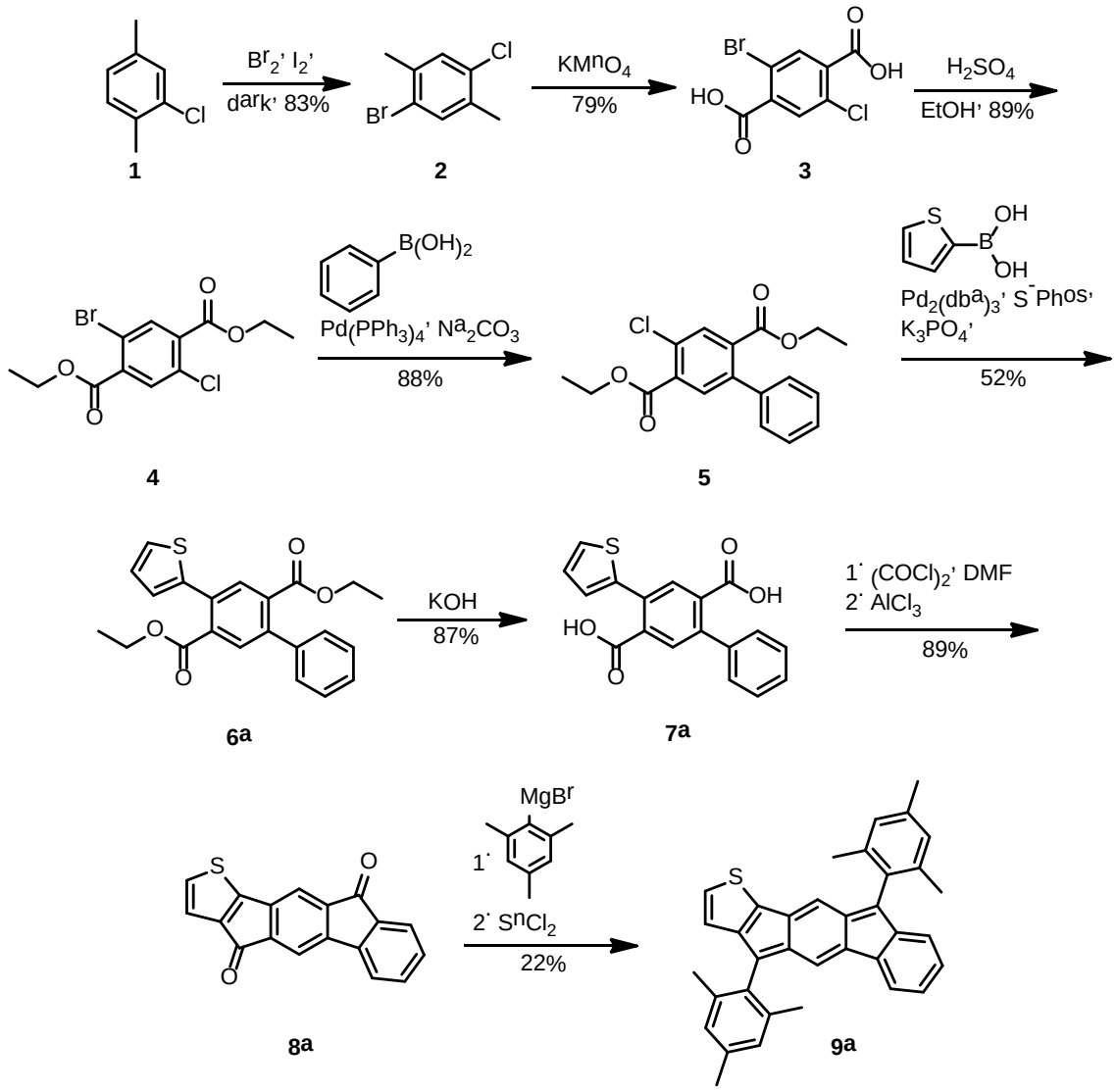

Figure 18: Complete synthesis of the *anti*- BIT isomer. *Syn*-isomer is not shown but follows the same general procedure.

The synthesis of the BITs began with the bromination of 2-chloro-para-xylene to produce brominated para-xylene **2**. This compound was oxidized with $KMnO_4$ to produce diacid **3**. Diacid **3** as well as the subsequent compounds were hitherto unknown in the literature. Fischer esterification of diacid **3** produced the core diester **4**. The bromine on diester **4** is more reactive towards oxidative addition than the chlorine.

Using modern cross-coupling techniques, we can selectively cross-couple onto either the bromine or chlorine. This compound (**4**) is of unique interest for its potential use in future asymmetric IF synthesis.

Mild Suzuki conditions were used to cross-couple phenylboronic acid onto diester **4**. This gratifyingly afforded the phenyl-coupled diester **5** in gram quantities. It should be noted that both 2- and 3-thienyl boronic acid cross-couplings were attempted at this same site. However, the simplest route was determined to be the phenyl cross-coupling before the thiophene addition. Diester **5** allowed for selective addition of 2- or 3-thienyl boronic acid onto the chlorine. Via Suzuki cross-coupling, the respective thienyl boronic acids were cross-coupled onto diester **5**, furnishing diesters **6a** and **6b**. Preliminary research suggests that any boronic acid or pinacol ester can be cross-coupled onto diesters **4** or **5** using the Suzuki conditions presented. Diesters **6a** and **6b** were saponified to provide the diacids **7a** and **7b**. Friedel-Crafts acylation of diacids **7a** and **7b** afforded the highly soluble diones **8a** and **8b**. Addition of mesityl Grignard produced the crude diols, which were in turn reacted with $SnCl_2$ to afford stable, purple crystals of BITs **9a** and **9b** in modest yields. Typical nucleophilic addition via a lithiate, in this case n-butyllithium, did not afford **9a** but instead produced **9c**. Although structurally similar to **9a**, **9c** has a C_4H_9 (butyl group) instead of a hydrogen attached to the carbon closest to the sulfur. This was determined via x-ray crystallography.

Further substitution at the 6 and 12 positions were attempted on dione **8a** using triisopropylsylil acetylene; however, the resulting deep purple product appeared to decompose upon concentration to afford a green decomposite. Further substitution onto

the **8b** was not attempted due to the reasonable conclusion that the similarity to the *anti*-isomer would produce the same decomposition.

Results and Characterization

Ultraviolet and Visible Light Spectroscopy

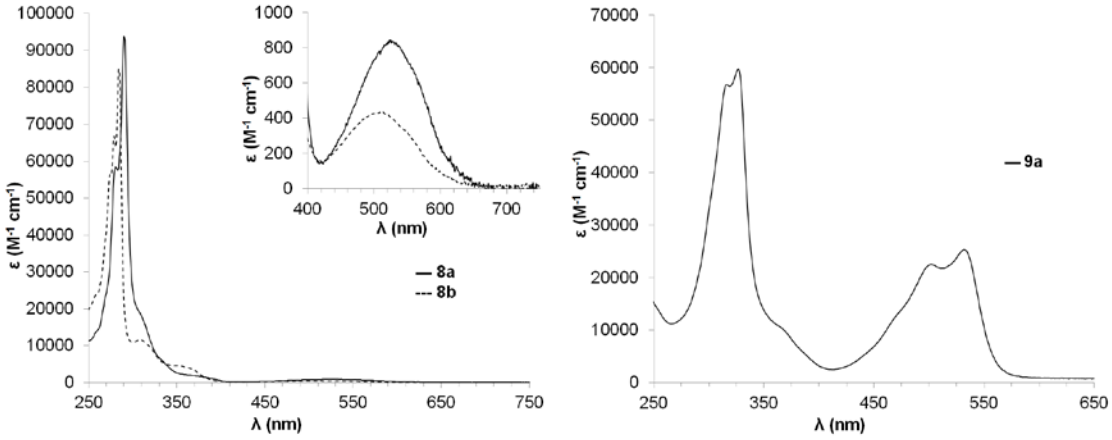

Figure 19: UV/Vis spectrums for 8a, 8b, and 9a. Peaks correspond to absorbances of light at particular wavelengths; the higher the peak, the more light that is absorbed. The longer wave absorptions are due to HOMO/LUMO interactions. Data gathered using an Agilent Technologies Cary 60 UV-Vis Spectrometer. Solvent: DCM.

The electronic absorption spectra of the diones **8a**, **8b**, and BIT **9a** are shown in Figure 19. The dione spectra display intense light absorptions from approximately 250-315 nm with broad absorption bands showing weak p-orbital electron transitions in the 450-600 nm range. Diones **8a** and **8b** have a λ_{max} at 524 nm and 512 nm, respectively. The spectrum of BIT **9a** shows intense absorptions from approximately 275 nm to 350 nm with broad absorptions bands in the 450-550 nm range with λ_{max} of 532 nm. As expected, these wavelengths fall between the spectra of the [1,2-b] IF and the IDTs (Table 1). Similar to the IDT absorption spectra, the *syn*-isomer for the BITs has lower

λ_{max} than the *anti*-isomer (15). We can also estimate the energy gap between the HOMO and LUMO levels using UV/Vis (14). BIT **9a** exhibits a band gap lower than the fully reduced IF yet higher than the fully reduced IDT. UV/Vis absorption data collection for BIT **9b** is still ongoing.

Table 1: Electrochemical and Optical data for diones **8a** and **8b**, BIT **9a**, reduced and oxidized IDTs, and reduced IF.

Compound	Electrochemical				Optical[b]	
	E_{red}^{1}(V)	E_{red}^{2} (V)	E_{HOMO} (eV)	E_{LUMO} (eV)	λ_{max} (nm)	E_{gap} (eV)
8a	–0.86	–1.29[c]	–	–3.78	524	2.00
8b	–0.83	–1.24[c]	–	–3.81	512	2.08
9a	–	–	–	–	532	2.21
Anti-IDT dione[a]	–0.91	-1.49	–	–3.73	566	1.75
Syn-IDT dione[a]	–0.87	–1.27	–	–3.77	551	1.89
Anti-IDT	–0.92	–1.69	–5.57	–3.72	561	2.07
Syn-IDT	–0.94	–1.59	–5.62	–3.70	592	1.96
IF	–1.12	–1.73	–5.78	–3.56	516	2.29

Values reported as the half-wave potential (vs SCE) using the Fc/Fc^{+} couple (0.46 V) as an internal standard. HOMO and LUMO energy levels in eV were approximated using SCE = -4.67 eV versus vacuum (see Ref. 13) and $E_{1/2}$ values for reversible processes. [a] Due to poor solubility in CH_2Cl_2, o-dichlorobenzene was used as a solvent for electrochemical measurements. [b] Spectra were obtained in CH_2Cl_2. The optical HOMO/LUMO gap was determined as the intersection of the x-axis and a tangent line passing through the inflection point of the lowest energy absorption. [c] Reported as V at peak current, not half-wave potential.

Cyclic Voltammetry

The diones **8a** and **8b** were assessed via CV and each displayed two reversible reductions, with no accessible oxidations inside the solvent window (Figure 20).

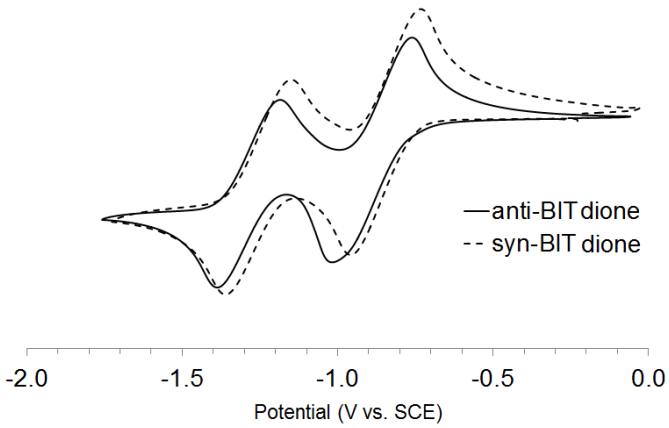

Figure 20: CVs were recorded using 1-5mM of analyte in 0.1 M Bu_4NBF_4/CH_2Cl_2 at a scan rate of 50 mV s^{-1} with a glassy carbon working electrode, a Pt coil counter electrode, and a Ag wire pseudo-reference.

Without the HOMO level, the difference in energy for the band gap cannot be determined from CV; however, LUMO levels can still be estimated from the first reduction (Table 1). We can see similar values for the BIT diones as for the IDT diones with a variation of only 0.04 eV for both the *anti*- and *syn*- isomers (Table 1) (15). CV data collection for **9a** and **9b** is still on going. However, data from the IDT diones compared to their fully conjugated versions suggests that the BIT reductions will result in an overall lower LUMO level than the diones. This is supported by the consistency of the data showing the BIT to behave has a hybrid between the IDTs and the IFs.

X-ray Diffraction

X-ray diffraction was also performed on the *anti*-BIT dione (**8a**) and fully conjugated *anti*-BIT (**9a**). We have so far been unable to isolate a crystal of either *syn*-BIT (**8b** or **9b**) suitable for x-ray diffraction. Crystal structures for **9a** shared similar characteristics with its predecessor the *anti*-IDT (15). Both crystal structures exhibit the same “herringbone” stacking motif (Figure 19).

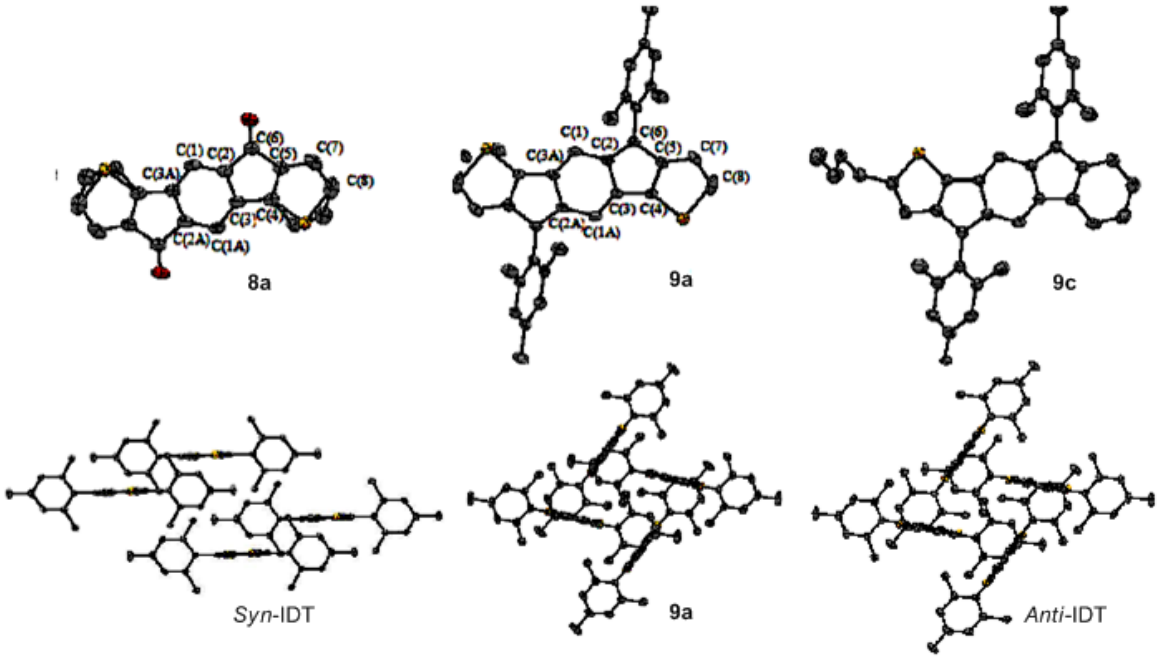

Figure 21: Crystal structures of dione 8a (top left) and 9a (top center) with numbered carbons for bond lengths in Table 2. The crystal structure for 9c is also presented (top right). Crystal packing for the *syn*-IDT (bottom left), *anti-IDT* (bottom right), and 9a (bottom center) are shown. Packing motifs are 1D - columnar packing and herringbone, respectively.

The similarities in the crystal structures as well as the similarities in the previous data between the BITs and the IDTs, suggest that the *syn*-BIT (**9b**) might have some favorable stacking given the distinct crystal structure of the *syn*-IDT favoring a parallel arrangement of the 1D columns (Figure 21). Upon further data collection, a definitive conclusion will be drawn. XRD also reveals that the bond lengths of **9a** also fall between the lengths of the *anti*-IDT and the IF (Table 2).

Table 2: Select Bond Lengths (Å) of **8a**, **9a**, *Anti*-IDT, *Syn*-IDT, and IF

Bond	$\mathbf{8_a}$	$\mathbf{10_a}$	*Anti*-IDT	*Syn*-IDT	IF
C1–C2	1.381	1.428	1.431	1.418	1.433
C1–C3A	1.391	1.361	1.360	1.363	1.356
C2–C3	1.411	1.460	1.469	1.456	1.467
C2–C6	1.506	1.384	1.388	1.398	1.380
C3–C4	1.464	1.456	1.452	1.461	1.469

Numbering scheme shown in Figure 21. C4–C8 bond lengths not shown as the fused ring is centrosymmetric.

It should be further noted that the crystal packing of both the *anti*-BIT dione and fully reduced compounds were disordered over two centrosymmetric points. This is significant because it implies that the dipole did not play a part during the solid packing of BIT **9a**. In other words, XRD observed an equal number of thiophenes and benzenes in the same average position within the unit cell, meaning there was no preferred alignment because of the dipole.

Concluding Remarks

Once more data is collected and the relationship between the *syn*- and *anti*-isomers, as well as the BITs and IDTs can be clarified, there will be more options for future research. The synthesis outlined in this thesis opens up the possibility for a variety of potential asymmetrical IFs. The next step in asymmetrical research will be to synthesize an asymmetrical IF with a stronger electron withdrawing group. This will allow for a better understanding of the dipole effect on these compounds. Electron

donating and accepting groups will also be asymmetrically added to the IF core, further influencing the electronic properties these compounds.

In the immediate future, the serendipitous discovery of the reactivity of the alpha-hydrogen on the thiophene of BIT **8a** (producing **9c**) has our research looking into the possibility of homo-coupling the asymmetric IFs. The properties of the resulting dimer will undoubtedly harbor valuable information for future OSC research.

Experimental Details

Air sensitive manipulations were performed using standard Schlenk line techniques. THF, toluene, and diethyl ether were refluxed with sodium benzophenone ketyl for 24 h prior to distillation. All other reagents were used without prior purification. 2-Thienyl boronic, 3-thienyl boronic, phenylboronic acid, tetrakis(triphenylphosphine)palladium(0), and tris(dibenzylideneacetone)dipalladium(0) were purchased from Sigma Aldrich. S-Phos (2-dicyclohexylphosphino-2',6'-dimethoxybiphenyl) was purchased from Matrix Chemicals. Chromatography was performed on 230-400 mesh silica gel purchased from Sigma Aldrich. NMR spectra were recorded on Varian Inova 500 (^{1}H: 500.11 MHz) or Inova 300 (^{1}H: 300 MHz) NMR spectrometer. Chemical shifts (δ) are expressed in ppm relative to the residual chloroform (^{1}H: 7.26 ppm) or dimethyl sulfoxide (^{1}H: 2.51ppm) as noted.

Synthesis

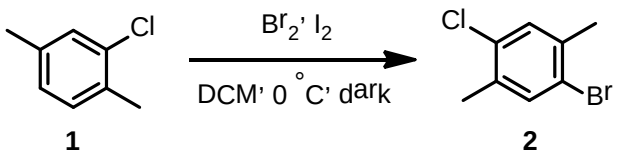

2-Bromo-5-chloro-1,4-dimethylbenzene 2: 2-Chloro-1,4-dimethylbenzene **1** (9.44 mL, 71.2 mmol, 1 equiv), iodine (9 mg, 0.356 mmol, 0.005 equiv), and DCM (100 mL) were degassed with N_2 for 15 min and cooled to 0 °C. After cooling, bromine (3.85 mL, 74.7 mmol, 1.05 equiv) was added dropwise to the reaction mixture and then stirred for 18 h in the dark while warming to rt. The reaction mixture was quenched with 10% KOH solution. The mixture was extracted 3x with DCM and 3x with brine, dried with $MgSO_4$ and filtered, the solvent was removed under reduced pressure. The crude product was recrystallized from EtOH to yield **2** (12.9 g, 83%) as white crystals. ^{1}H NMR (300 MHz, $CDCl_3$) δ 7.41 (s, 1H), 7.22 (s, 1H), 2.35 (s, 3H), 2.33 (s, 3H).

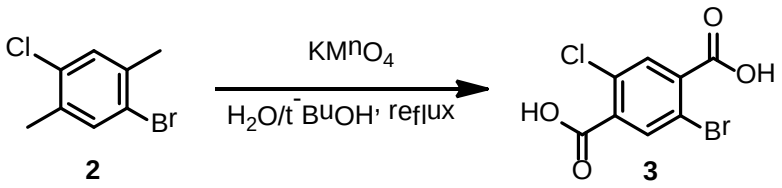

1-Bromo-4-chloroterepthalic acid 3: 2-Bromo-5-chloro-1,4-dimethylbenzene **2** (5.01 g, 22.78 mmol, 1 equiv), $KMnO_4$ (7.92 g, 50.1 mmol, 2.2 equiv), H_2O (37.5 mL), t-BuOH (37.5 mL) were stirred at reflux for 1 hour. The reaction mixture was cooled to rt and $KMnO_4$ (7.92 g, 50.1 mmol, 2.2 equiv) was added. The mixture was refluxed for 18 h. After cooling, the reaction mixture was filtered using vacuum filtration. The diacid was precipitated from the filtrate by careful addition of concentrated HCl solution to

yield **3** (5.02 g, 79%) as a white solid. ^{1}H NMR (300 MHz, DMSO-d_6) δ 14.1 (br s, 2H), 8.06 (s, 1H), 7.87 (s, 1H).

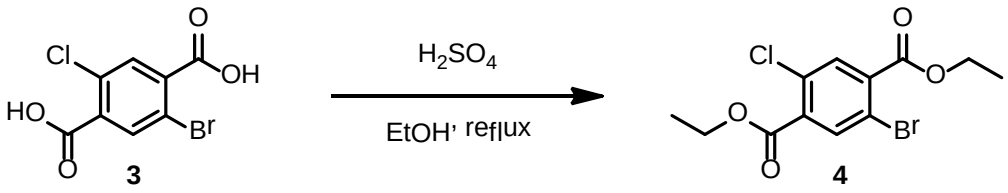

Diethyl 2-bromo-5-chloroterepthalate 4: 2-Bromo-5-chloroterephthalic acid **3** (4.98 g, 15.4 mmol, 1 equiv), H_2SO_4 (18.4 M, 16.78 mL, 309 mmol), and EtOH (125 mL) were stirred at reflux 18 h. After cooling, EtOH was removed under reduced pressure. The reaction mixture was diluted with saturated $NaHCO_3$ and carefully neutralized with KOH. The precipitate was collected via vacuum filtration and then dissolved in DCM. The DCM was dried with $MgSO_4$, filtered, and the solvent was removed under reduced pressure to afford the diester **4** (4.60 g, 89%) as white solid. ^{1}H NMR (300 MHz, $CDCl_3$) δ 8.10 (s, 1H), 7.86 (s, 1H), 4.446 (q, J = 7.2 Hz 2H), 4.444 (q, J = 7.1 Hz, 2H), 1.444 (t, J = 7.1 Hz, 3H), 1.441 (t, J = 7.1 Hz, 3H).

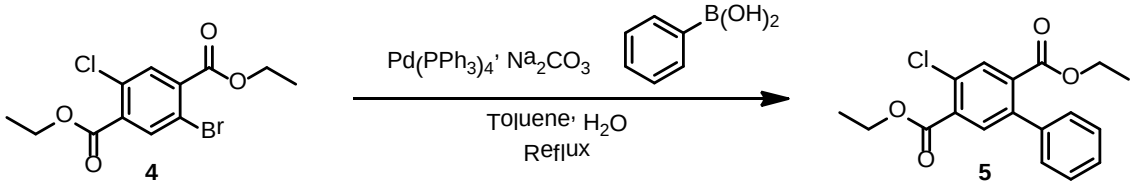

Diester 5: Diethyl 2-bromo-5-chloroterephthalate **4** (4.64 g, 13.8 mmol, 1 equiv), phenylboronic acid (2.02 g, 16.6 mmol, 1.2 equiv), Na_2CO_3 (2.93 g, 27.6 mmol, 2 equiv), H_2O (25 mL), and toluene (225 mL) were stirred and degassed for 30 min with

N_2. Tetrakis(triphenylphosphine)palladium (0.319 g, 0.276 mmol, 0.02 equiv) was then added and degassed for a further 10 min. The reaction mixture was then stirred at reflux for 18 h. After cooling, the reaction mixture was quenched with H_2O, extracted 3x with Et_2O and brine, dried with $MgSO_4$, and the solvent was removed under reduced pressure. The product was purified via silica gel chromatography (9:1 hexanes:EtOAc) to provide **5** (4.03 g, 88%) as a colorless highly viscous oil. ^{1}H NMR (300 MHz, $CDCl_3$) δ 7.76 (s, 1H), 7.67 (s, 1H), 7.32–7.12 (m, 5H), 4.29 (q, J = 7.0 Hz, 2H), 3.98 (q, J = 7.1 Hz, 2H), 1.27 (t, J = 7.0 Hz, 3H), 0.89 (t, J = 7.1 Hz, 3H).

Anti-BIT Synthesis

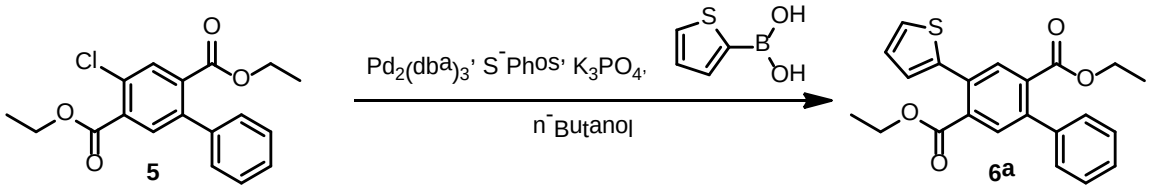

Diester 6a: Diester **5** (2 g, 5.99 mmol, 1 equiv), 2-thienylboronic acid (1.15 g, 8.99 mmol, 1.5 equiv), SPhos (0.195 g, 0.479 mmol, 0.08 equiv), K_3PO_4 (2.54 g, 11.9 mmol, 2 equiv), and n-butanol (175 mL) were stirred and degassed with N_2 for 30 min. Tris(dibenzylideneacetone)dipalladium (0.03 g, 0.15 mmol, 0.02 equiv) was added to the reaction mixture and the resulting solution was degassed for an additional 10 min. The solution was left at reflux for 18 h. After cooling, the reaction mixture was quenched with H_2O, extracted 3x with Et_2O, and washed 3x brine, dried with $MgSO_4$ and filtered. The solvent was removed under reduced pressure and the product was purified via recrystallization in EtOH to yield **6a** (1.21 g, 52%) as a white solid. ^{1}H

NMR (300 MHz, $CDCl_3$) δ 7.93 (s, 1H), 7.73 (s, 1H), 7.46–7.34 (m, 5H), 7.14–7.07 (m, 3H), 4.18 (apparent t, J = 6.6 Hz, 2H), 4.08 (apparent t, J = 6.5 Hz, 2H), 0.88 (t, J = 7.3 Hz, 3H), 0.82 (t, J = 7.3 Hz, 3H).

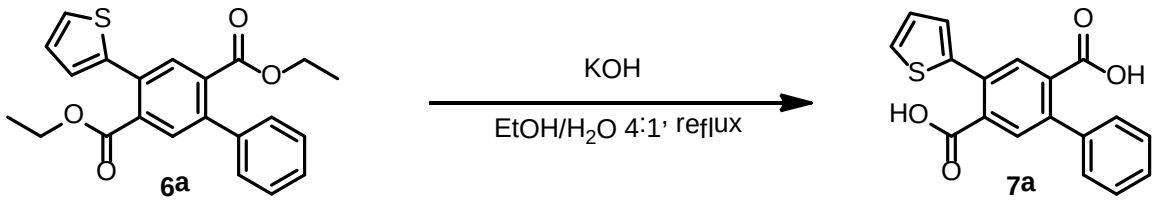

Diacid 7a: Diester **6a** (1.21 g, 3.17 mmol, 1 equiv), KOH (2.84 g, 50.9 mmol, 16 equiv), H_2O (25.5 mL) and EtOH (97.5 mL) were stirred at reflux for 18 h. After cooling, the EtOH was removed under reduced pressure. The reaction mixture was diluted with H_2O and acidified carefully using concentrated HCl. The precipitate was collected and recrystallized in EtOH to yield **7a** (0.905 g, 87%) as a white solid. ^{1}H NMR (300 MHz, DMSO-d_6) δ 13.30 (br s, 2H), 7.80 (s, 1H), 7.69 (d, J = 5.2 Hz, 1H), 7.61 (s, 1H), 7.48–7.37 (m, 5H), 7.27 (d, J = 3.5 Hz, 1H), 7.17 (t, J = 4.4 Hz, 1H).

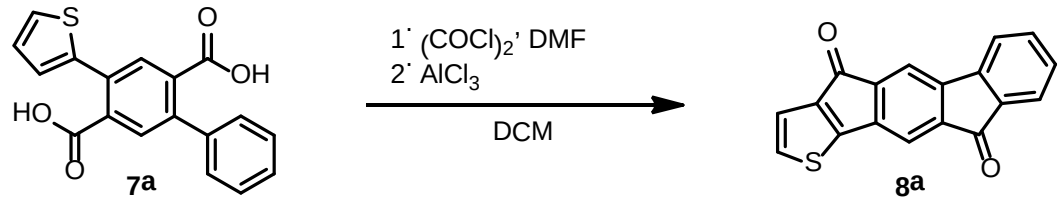

Dione 8a: To an air-free, oven-dried round bottom flask were added diacid **7a** (0.8 g, 2.45 mmol, 1 equiv), oxalyl chloride (0.84 mL, 10.9 mmol, 4 equiv) and dry DCM (40 mL). After cooling to 0 °C, dimethylformamide (0.38 mL, 4.9 mmol, 2 equiv) was

added under N_2 to the reaction mixture. This was allowed to warm to rt while stirring overnight. In the morning, the solvent was removed under reduced pressure, the mixture was placed under N_2 and suspended in dry DCM (40 mL) under N_2. Solid $AlCl_3$ (1.54 g, 11.5 mmol, 4.7 equiv) was added, the reaction mixture was stirred at rt overnight. The reaction mixture was then poured into a 1:1 10% HCl and ice mixture to precipitate the dione. The precipitate was collected via vacuum filtration and washed with H_2O to afford **8a** (0.635 g, 90%) as a dark blue solid. ^{1}H NMR (500 MHz, $CDCl_3$) δ 7.70–7.66 (m, 1H), 7.58–7.52 (m, 1H), 7.46 (s, 1H), 7.36 (apparent t, 7.1 Hz 1H), 7.30–7.24 (m, 2H), 7.20 (d, 4.8 Hz,1H), 7.17 (d, 4.9 Hz, 1H).

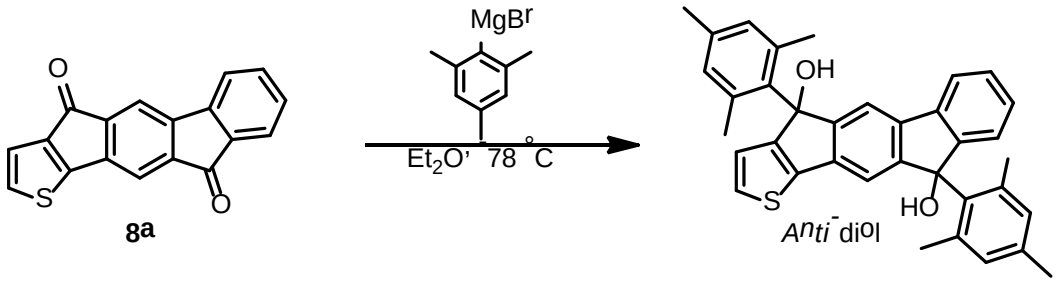

***Anti*-diol:** A mixture of dione **8a** (100 mg, 0.35 mmol, 1 equiv) and THF (25 mL) under N_2 was cooled to –78 °C. Mesitylmagnesium bromide (1.0M, 1.73 mL, 1.73 mmol, 5 equiv) was slowly added and the reaction mixture was stirred 18 h while warming to room temperature. A 1:1 ratio of 10% HCl solution and ice were used to quench the reaction to afford a red-orange solution. The mixture was extracted 3x with Et_2O and washed 3x with brine, dried with $MgSO_4$ and filtered. The solvent was removed under reduced pressure to afford crude *anti*-diol that was carried on without further purification or characterization.

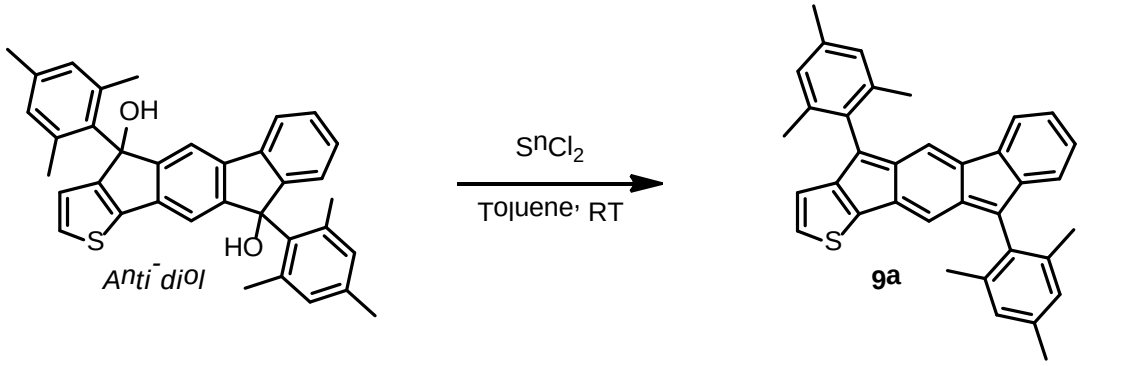

BIT 9a: Crude *anti*-diol (367 mg, 0.69 mmol, 1 equiv), $SnCl_2$ (526 mg, 2.8 mmol, 4 equiv), and toluene (25 mL) were combined in a flask under N_2. The reaction mixture was stirred for 18 h and washed over a pad of silica (2:1 hexanes:DCM). The solvent was removed under reduced pressure and recrystallized in chlorobenzene to afford BIT **9a** (77.2 mg, 22%) as a dark red solid. ^{1}H NMR (300 MHz,$CDCl_3$) δ 7.14 (d, J = 7.3 Hz, 1H), 7.00 (s, 4H), 6.96-6.89 (m, 2H), 6.83 (apparent t, J = 7.6 Hz, 1H), 6.59 (d, J = 7.6 Hz, 1H), 6.53 (s, 1H), 6.48 (s, 1H), 6.39 (d, J = 4.8 Hz, 1H), 2.38 (s, 6H), 2.28 (s, 6H), 2.19 (s, 6H).

Syn-BIT Synthesis

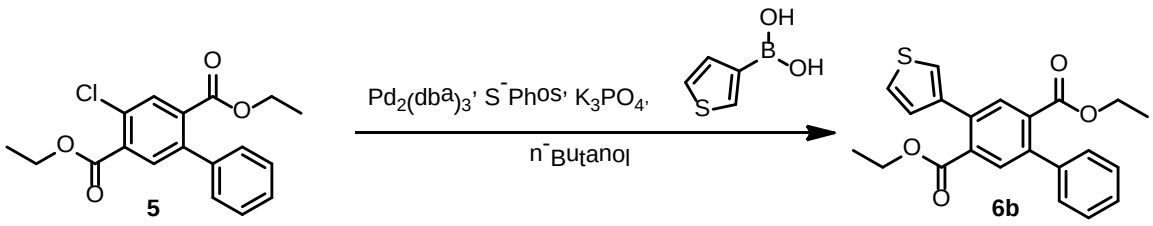

Diester 6b: Diester **5** (1.6 g, 4.80 mmol, 1 equiv), 3-thienylboronic acid (0.92 g, 7.20 mmol, 1.5 equiv), SPhos (0.16 g, 0.38 mmol, 0.08 equiv), K_3PO_4 (2.32 g, 9.59 mmol, 2 equiv), and n-butanol (125 mL) were stirred and degassed with N_2 for 30 min.

Tris(dibenzylideneacetone)dipalladium (0.02 g, 0.096 mmol, 0.02 equiv) was added to the reaction mixture and degassed with N_2 for a further 10 min. The solution refluxed for 18 h. After cooling the reaction mixture was quenched with H_2O, extracted 3x with Et_2O and 3x with brine, dried with $MgSO_4$, and filtered. The solvent was removed under reduced pressure and the product was purified via recrystallization in EtOH to yield **6b** (0.66 g, 40%) as white crystals. ^{1}H NMR (300 MHz, $CDCl_3$) δ 7.86 (s, 1H), 7.80 (s, 2H), 7.76 (s, 1H), 7.44–7.31 (m, 5H), 7.15 (dd, J = 4.9, 1.4 Hz, 2H), 4.15 (apparent t, J = 6.6 Hz, 4H), 4.06 (apparent t, J = 6.5 Hz, 2H), 0.86 (t, J = 7.4 Hz, 5H), 0.80 (t, J = 7.3 Hz, 3H).

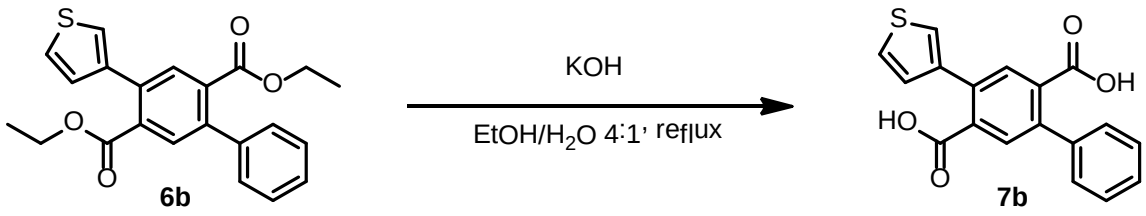

Diacid 7b: Diester **6b** (0.83 g, 2.17 mmol, 1 equiv), KOH (1.95 g, 34.7 mmol, 16 equiv), H_2O (17 mL) and EtOH (85 mL) were stirred and refluxed at 110 °C for 18 h. After cooling, the EtOH was removed under reduced pressure. The reaction mixture was diluted with H_2O and acidified carefully using concentrated HCl. The precipitate was collected to yield **7b** (0.697 g, 98%) as a while solid. ^{1}H NMR (500 MHz, DMSO-d_6) δ 13.16 (br s, 2H), 7.77 (s, 1H), 7.68 (d, 6.9 Hz, 2H), 7.63 (s, 2H), 7.50–7.37 (m, 4H), 7.24 (d, 4.7 Hz, 1H).

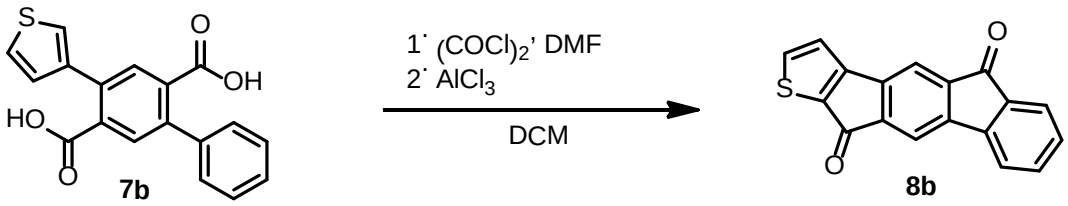

Dione 8b: Diacid **7b** (0.943 g, 2.89 mmol, 1 equiv), oxalyl chloride (0.99 mL, 11.5 mmol, 4 equiv) and dry DCM (40 mL) were stirred and cooled to 0 °C under N_2. Dimethylformamide (0.49 mL, 5.77 mmol, 2 equiv) was added to the reaction mixture and stirred 18 h. The solvent was removed under reduced pressure. The mixture was then suspended in dry DCM (40 mL) under N_2. $AlCl_3$ (1.81 g, 13.6 mmol, 4.7 equiv) was added and the reaction mixture was stirred for 18 h. The reaction mixture was then poured into a 1:1 10% HCl and ice mixture to precipitate the dione. The precipitate was collected via vacuum filtration and washed with H_2O to afford **8b** (0.721 g, 86%) as a dark green solid. ^{1}H NMR (500 MHz, $CDCl_3$) δ 7.86 (d, 4.7 Hz, 1H), 7.82 (d, 4.7 Hz, 1H), 7.68–7.66 (m, 1H), 7.57–7.51 (m, 1H), 7.49 (s, 1H), 7.37–7.32 (m, 1H), 7.19 (d, 4.7 Hz, 1H), 7.15 (d, 4.7 Hz, 1H).

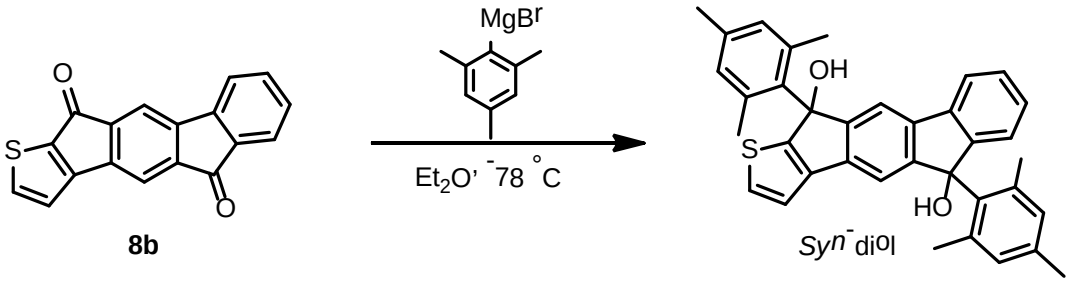

***Syn*-diol:** A mixture of dione **8b** (100 mg, 0.35 mmol, 1 equiv) and THF (25 mL) under N_2 was cooled to –78 °C. Mesitylmagnesium bromide (1.0 M, 1.73 mL, 1.73 mmol, 5 equiv) was slowly added and the reaction mixture was stirred 18 h. A 1:1 ratio of 10%

HCl solution and ice were used to quench the reaction to afford a red-orange solution. The mixture was extracted 3x with Et_2O and washed 3x with brine, dried with $MgSO_4$, filtered, and the solvent was removed under reduced pressure to afford the crude *syn*-diol that was carried on without further purification or characterization.

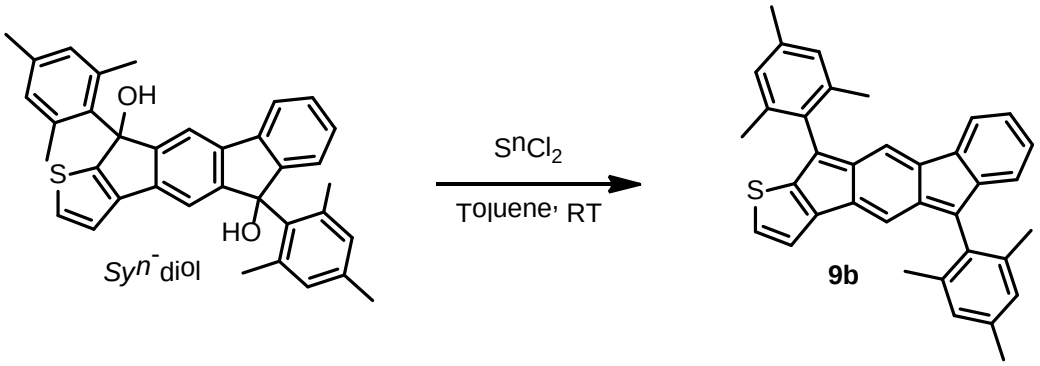

BIT 9b: Crude *syn*-diol (30 mg, 0.09 mmol, 1 equiv), $SnCl_2$ (69.2 mg, 0.37 mmol, 4 equiv), and toluene (25 mL) were combined in flask under N_2. The reaction mixture was stirred for 18 h and washed over a pad of silica (2:1 hexanes:DCM) to afford BIT **9b** (7.1 mg, 16%) as a dark purple solid. NMR data analysis is ongoing.

Butylated Anti-BIT Synthesis

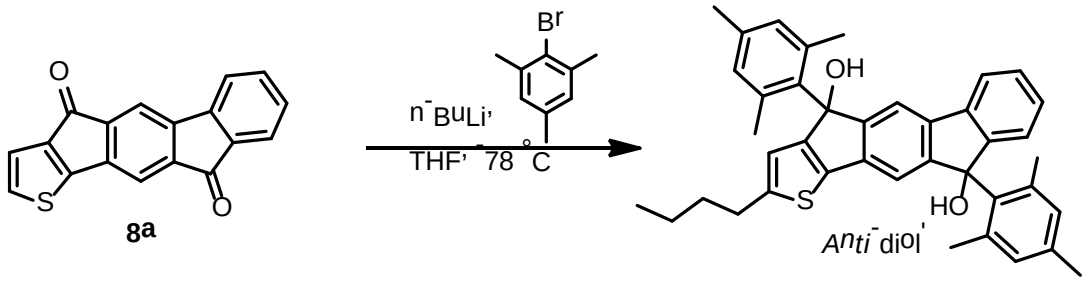

***Anti*-diol':** Dione **8a** (100 mg, 0.35 mmol, 1 equiv), and THF (25 mL) were added to an under N_2 and cooled to –78 °C. Mesityl bromide (0.26 mL, 2.13 mmol, 6 equiv), n-

butyllithium (2.5M, 0.68 mL, 1.77 mmol, 5 equiv), and THF (25 mL) were added to an oven-dried round bottom flask and cooled to –78 °C. After 1 h, the reaction mixture was added to the flask containing the dione **8a** suspended in THF. The resulting mixture was stirred 18 h. A 1:1 ratio of 10% HCl solution and ice were used to quench the reaction to afford a red-orange solution. The mixture was extracted 3x with Et_2O and washed 3x with brine, dried with $MgSO_4$, filtered, and the solvent was removed under reduced pressure to afford the crude *anti*-diol' that was carried on without further purification or characterization.

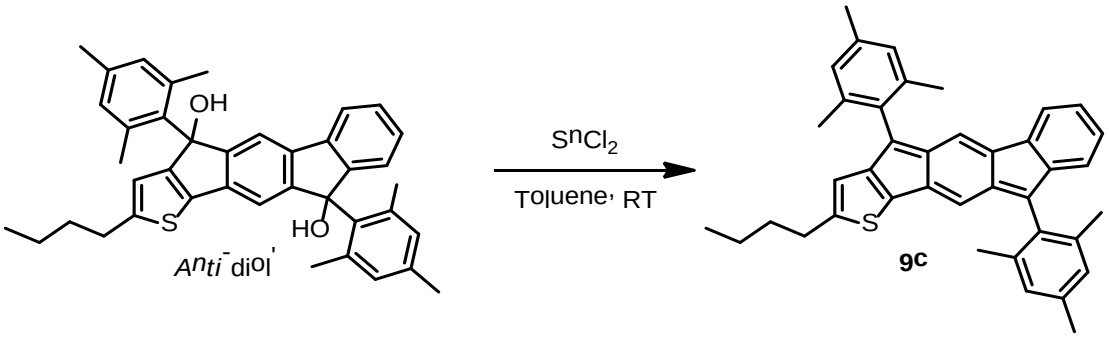

BIT 9c: Crude an*ti*-diol' (367 mg, 0.69 mmol, 1 equiv), $SnCl_2$ (526 mg, 2.77 mmol, 4 equiv), and toluene (25 mL) were combined in an oven-dried round bottom flask under N_2. The reaction mixture was stirred for 18 h and washed over a pad of silica (4:1 DCM:hexanes) to afford BIT **9c** (0.19 g, 27% yield) as a dark red solid. ^{1}H NMR (300 MHz, $CDCl_3$) δ 7.09 (d, J = 7.3 Hz, 1H), 6.99 (s, 2H), 6.98 (s, 2H), 6.90 (apparent t, J = 7.2 Hz, 1H), 6.81 (apparent t, J = 7.1 Hz, 1H), 6.56 (d, J = 7.4 Hz, 1H), 6.46 (s, 1H), 6.35 (s, 1H), 6.09 (s, 1H), 2.62 (t, J = 7.6 Hz, 1H), 2.38 (s, 3H), 2.37 (s, 3H), 2.28 (s, 6H), 2.19 (s, 6H), 1.56 (t, J = 7.5 Hz, 1H), 1.34 (q, J = 7.5 Hz, 1H), 0.89 (t, J = 7.3 Hz, 1H).

Glossary

The following terms may not be familiar to the reader. They hey have been defined here to the extent relevant for this project.

Aromatic: Term given to cyclic organic compounds that have “4n+2” electrons in their pi systems, where “n” is an integer.

Conduct: The ability to transfer electrons.

Current: Flow of electric charge.

Charge: When neutrality is disrupted by the presence or lack of presence of an electron. More electrons = negative charge, less electrons = positive charge.

Density: The amount of population in a given space, often measured using mass/volume.

Electron: Negatively charged particle that occupies the outside of an atom, attracted to the positively charged proton core.

Electron Acceptor: These are single or multi element structures that are exceptional at adding electrons to its system, generally made up of elements with high **electronegativity.**

Electron Donor: These are single or multi element structures that are exceptional at giving up electrons, generally made up of elements with low **electronegativity**.

Electronegativity: Experimental value representative of how much an element “attracts” electrons.

Electron Transfer: What occurs when an electron moves from one atom to another, either through single atoms, or through a molecule.

Fourier Transform: Mathematical function used to decompose signals into its constituent frequencies.

Free Rotation: The ability to turn about an axis (the bond) without impediment.

Functionalization: The activity of manipulating a molecular structure through additions or changes to or of its atoms.

Hole: The lack of an electron in a system, considered to be a positive charge from a physics point of view.

Intra-molecularly: Within a chemical structure.

Inter-molecularly: Between two or more chemical structures.

Isomer: A compound is considered an isomer if it has the same chemical formula but a different structure.

Kinetic: Caused by motion, compounds can be kinetically stabilized via the restriction of movement.

Orbitals: Probability that electrons are occupying a given space at a given time. These are depicted as oval in shape, often similar to the form of an "8" where the cross section is the center of the atom.

Organic: Any carbon based structure, always involving carbon and often, nitrogen, oxygen, hydrogen, and sulfur.

Oxidation: Process of losing electrons.

Pi System: Electrons in the conjugated p-orbitals of a molecule.

Potential: Amount of work done by an electric field.

Reduction: Process of gaining electrons.

Scaffold: Basic structure that offers a lot of sites for "tuning", see **tuning sites**.

Solvate: To dissolve a compound in a liquid, one solvates something to create a solution.

Sterics: The reduction of kinetic movement in and around a molecular structure. A sterically bulky group reduces the amount of flexibility, rotation, and access of/to a molecule.

Tuning Sites: Locations on a chemical structure that can be altered with various elements/compounds, done to make small changes to the properties of the molecule.

Unit Cell: The smallest area of volume that contains all of the structural and symmetry information of a molecular structure.

Van der Waal's radius: The distance at which atomic particles interact.

Bibliography

(1) Neamen, D. A.; Boris, P. *Semiconductor Physics and Devices: Basic Principles*. Vol. 3. McGraw-Hill: NY, **2003**.

(2) Schubert, E. F, ed. *Delta-doping of Semiconductors*. Cambridge University Press: Cambridge, UK, **1996**.

(3) Aleksic, J.; Paul Z.; Janusz A. S. *Ann. New York Acad. Sci.* **2002**, 972,158-163.

(4) Petrucci, R. H., Harwood, W. S., Herring, G. F., Madura, J. D. *General Chemistry:Principles and Modern Applications*. Pearson Education International. Canada, **2007**.

(5) Nomura, K. et al. *Nature* **2004**, *432*, 488-492.

(6) Marshall, J. L.; Haley, M. M. *Organic Redox Systems: Synthesis, Properties and Applications*; Nishinaga, T., Ed.; Wiley-Blackwell: NY, in press.

(7) McQuarrie, D. A.; Simon, J. D. *Physical Chemistry: a Molecular Approach*. Vol 1, University Science Books: Sausalito, CA, **1997**.

(8) West, A. R. *Basic Solid State Chemistry*. John Wiley & Sons Inc.: NJ, **1999**.

(9) Anslyn, E. V.; Dougherty D. A. *Modern Physical Organic Chemistry*. University Science Books: CA, **2006.**

(10) Maitland, J. Jr,; Fleming, S. A. *Organic Chemistry*. W.W. Norton & Company, Inc.: NY, **2010.**

(11) Anthony, J. E. *Chem. Rev.* **2006**, *106*, 5028-5048.

(12) Keeler, J. *Understanding NMR Spectroscopy*. John Wiley & Sons: NJ, **2011**.

(13) Bard, A. J.; Faulkner L. R. *Electrochemical Methods: Fundamentals and Applications*, Vol. 2, Wiley: NY, **1980**.

(14) Ashkan, S.; Salleh M. M.; Yahaya, M. *Sains Malaysiana* **2011**, *40*, 173-176.

(15) Young, B. S.; Chase, D. T.; Marshall, J. L.; Vonnegut, C. L.; Zakharov, L. N.; Haley, M. M. *Chem. Sci.* **2014**, *5*, 1008-1014.

(16) Gabriel, S. *Ber. Dt. Chem. Ges.* **1884**, *17*, 1389.

(17) Chardonnens, L.; Salamin, L. *Helv. Chim. Acta* **1968**, *51*, 1096.

(18) Deuschel, W. *Helv. Chim. Acta* **1951**, *35*, 2403.

(19) Zhou, Q.; Carroll, P. J.; Swager, T. M. *J. Org. Chem.* **1994**, *59*, 1294-1301.

(20) Miyata, Y.; Minari, T.; Nemoto, T.; Isoda S.; Komatsu, K. *Org. Biomol. Chem.* **2007**, *5*, 2592-2598.

(21) Merlet, S.; Birau, M.; Wang, Z. Y. *Org. Lett.* **2002**, *4*, 2157-2160.

(22) Chase, D. T.; Fix, A. G.; Rose, B. D.; Weber, C. D.; Nobusue, S.; Stockwell, C. E.; Zakharov, L. N.; Lonergan, M. C.; Haley, M. M. *Angew. Chem. Int. Ed.* **2011**, *50*, 11103-11106.

(23) Chase, D. T.; Fix, A. G.; Kang, S. J.; Rose, B. D.; Weber, C. C.; Zhong, Y., Zakharov L. N.; Lonergan, M. C.; Nuckolls, C.; Haley, M. M. *J. Am. Chem. Soc.* **2012**, *134*, 10349-10352.

Image Sources

(1') Retrieved from: http://excelmodeljetsclub.blogspot.com/p/periodic-table-of-elements.html

(2') Retrieved from: http://en.wikipedia.org/wiki/Cyclic_voltammetry